

SUPPLEMENTARY INFORMATION

Histidine orientation in artificial peroxidases as determined by paramagnetic NMR shifts.

Ornella Maglio,^{a,b} Marco Chino,^a Claudia Vicari,^a Vincenzo Pavone,^a

Ricardo O. Louro,^{*c} and Angela Lombardi^{*a}

^aDepartment of Chemical Sciences, University Federico II of Naples, Via Cintia 21, 80126, Naples, Italy. alombard@unina.it

^bIBB-CNR, Via Mezzocannone 16, 80134, Naples, Italy.

^cITQB-UNL, Av. da Republica (EAN), 2780-157 Oeiras, Portugal. louro@itqb.unl.pt

Table of Contents

Figure S1		3
Section S1	Materials, Equipment and Methods	4
Section S2	Peptides Synthesis and Purification	6
Section S3	CD Analysis	12
Section S4	NMR Characterization	16
Section S5	Binding Properties by UV-Vis spectroscopy	18
Section S6	Stopped-Flow kinetic analysis	21
Section S7	References	23

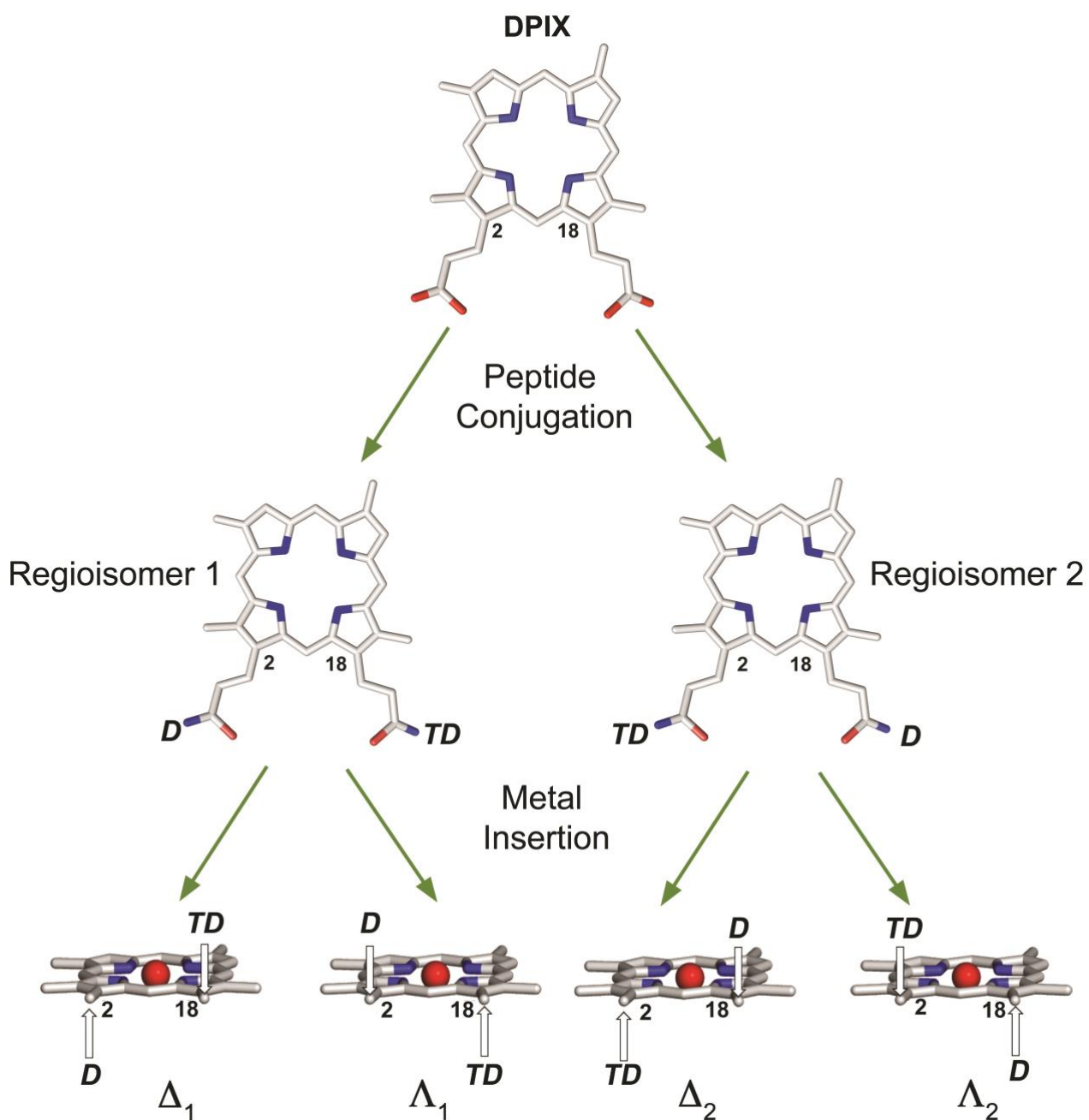


Figure S1. Schematic representation of MC6*a regioisomers and diastereoisomers formation. The decapeptide chain and the tetradecapeptide chain are indicated as D and TD, respectively. The metal ion is shown as red sphere.

Section S1: Materials, Equipment and Methods

✓ *Materials*

All 9-fluorenylmethoxycarbonyl (Fmoc) protected amino acids, Nova Syn TG Sieber resin and coupling reagents: N-hydroxybenzotriazole (HOBt), O-7-Azabenzotriazol-1-yl- N,N,N',N''-tetramethyluronium hexafluorophosphate (HATU) and benzotriazole-1-oxo- tris-pyrrolidino-phosphonium hexafluorophosphate (PyBOP) were purchased from NovaBiochem (EMD Biosciences, La Jolla, CA). Silica gel 60 (230-400 mesh) was from Merck. Precoated silica G-60 plates, F254, were used for thin-layer chromatography (tlc). 96-well plates were purchased from B D FALCON™.

All solvents used in the peptide synthesis and purification were anhydrous and HPLC grade respectively, and were supplied by Romil. Piperidine and scavengers (ethanedithiol, triisopropylsilane) were from Fluka. N,N-Diisopropylethylamine (DIPEA), trifluoroacetic acid (TFA) were supplied from Applied Biosystems. N,N-dimethylformamide (DMF), dichloromethane (DCM), pyridine, ethanol, methanol and 1-methyl-2-pyrrolidone (NMP) were supplied by Romil. Deuteroporphyrin IX was from Porphyrin Products. Iron(II) acetate was purchased from Sigma Aldrich. Solvent mixtures are indicated in the respective sections.

✓ *Equipment and Methods*

Peptide synthesis was performed using ABI 433 automatic peptide synthesizer (Applied Biosystems, Foster City, CA, USA).

HPLC and LC-MS analysis were performed with a Shimadzu LC-10ADvp equipped with an SPD10Avp diode-array detector.

Purifications were performed on a C18 column (250 mm x 5 cm) at 100 mL/min flow rate.

ESI-MS spectra were recorded on a Shimadzu LC-MS-2010EV system with ESI interface, Q-array-octapole-quadrupole mass analyzer, and Shimadzu LC-MS solution Workstation software for data processing. The optimized MS parameters were selected as followed: CDL (curved desolvation line) temperature 250 °C; heat block temperature 250 °C; probe temperature 250 °C; detector gain 1.6kV; probe voltage +4.5kV; CDL voltage -15V. Nitrogen served as the nebulizing gas (flow rate: 1.5 L/min).

Flash chromatography was performed with a Biotage Isolera flash purification system, equipped with a diode-array detector.

UV-vis spectra were recorded on Cary Varian 50 Probe UV Spectrophotometer equipped with a thermostated cell holder and a magnetic stirrer. Quartz cuvettes with a path length of 1.0 cm were used. Wavelength scans were performed at 25°C from 200 to 800 nm. All data were blank subtracted. Fe-Lys9DabMC6*a-1 and Fe-Lys9DabMC6*a-2 concentrations were determined by UV/Vis spectroscopy, using $\epsilon_{389} = 1.50 \times 10^5 \text{ M}^{-1}\text{cm}^{-1}$, and $1.80 \times 10^5 \text{ M}^{-1}\text{cm}^{-1}$ (H₂O, 0.1% TFA v/v), respectively.

CD measurements were carried out on Jasco J-815 dichrograph, equipped with a thermostated cell holder (JASCO, Easton, MD, USA).

CD spectra were collected at 25°C, from 260 to 190 nm in the far UV region and from 460 to 300 nm in the Soret region, at 0.2 nm intervals with a 20 nm min⁻¹ scan speed, at 1 nm bandwidth and at 16 s response. In order to improve signal to noise ratio, spectra, in the Soret region, were averaged on 5 accumulations.

Far-UV CD spectra were collected at 5.0·10⁻⁶ M in phosphate buffer 20 mM (pH 5.0) at various TFE concentrations. CD spectra in the Soret region were collected at 1.5·10⁻⁵ M in phosphate buffer 10 mM (pH 5.0) at various TFE concentrations.

Kinetic parameters were measured, as previously described,¹ using a stopped flow instrument SX20 from Applied Photophysics in double mixing mode.

All NMR experiments were performed as previously described² at 500.13MHz in a Bruker Avance II spectrometer using 3.0 10⁻⁴ M and 3.5 10⁻⁴ M solutions of mixed buffer 60/40 of 60 mM phosphate buffer pH 5.8/TFE for Fe-Lys⁹DabMC6*a-1 and Fe-Lys⁹DabMC6*a-2, respectively. Briefly, NOESY experiments were collected with 25 and 80 ms mixing time and 400 ms water pre-saturation during relaxation delay; ¹H-¹³C-HMQC experiments were collected using samples in natural abundance with 300 ms water pre-saturation during relaxation delay and decoupling during acquisition. Data were processed using the Topspin 3.2 software from Bruker.

The detailed synthetic procedures are reported in the following sections.

✓ *Synthesis of protected peptides*

All the peptides were obtained by solid-phase synthesis, using the Fmoc protection strategy.

The following amino acids were used:

TD: Fmoc-Asp(OtBu)-OH; Fmoc-Leu-OH; Fmoc-Gln(Trt)-OH; Fmoc-His(Trt)-OH; Fmoc-Ser(tBu)-OH; Fmoc-Lys(Mmt)-OH; Fmoc-Arg(Pbf)-OH; Fmoc-Lys(Boc)-OH; Fmoc-Ile-(OH); Fmoc-Thr(tBu)-OH;

Lys⁹Dab-D: Fmoc-Asp(OtBu)-OH; Fmoc-Glu(OtBu)-OH; Fmoc-Aib-OH; Fmoc-Gln(Trt)-OH; Fmoc-Leu-OH; Fmoc-Ser(tBu)-OH; Fmoc-Dab(Mtt)-OH; Fmoc-Arg(Pbf)-OH.

A super acid labile NovaSyn[®] TG Sieber (0.62 mmol/g loading) was chosen for the synthesis, because it allows the cleavage of the fully protected peptide chains under very mild conditions.³ Once the Fmoc group was removed from the resin, cyclic coupling, capping and deprotection steps were repeated with each amino acid, until the chain assembly was completed. At the end of the solid-phase synthesis, the resin was washed with NMP and the peptides, amidated at the C-terminus, were finally acetylated at the N-terminus with Ac₂O/HOBt/DIPEA solution in NMP.

✓ *Mtt deprotection and cleavage of the protected peptides*

Once peptide synthesis was completed, simultaneous cleavage of peptides from resin, Mmt (4-methoxytrityl) deprotection of the ϵ amino group of Lys⁹ and Mtt (4-methyltrityl) deprotection of γ amino group of Dab⁹ were performed.

The removal of the N- ϵ Mmt protecting group from the Lys⁹ side chain and the cleavage of the tetradecapeptide from the resin were performed as previously described by us (Caserta et al., 2018). The N- γ Mtt side chain protecting group of the Dab⁹ was removed by repeated treatments (1 hour) with a solution containing DCM:HFIP:TFE:TES 6.5:2.0:1.0:0.5 (v/v). Every hour few beads of resin were taken off, 1-2 drops of TFA were added and the color of the resin was checked. The step was repeated until no orange color was detected for the beads. Then, the resin was filtered, washed twice with DCM, DMF, 10% DIPEA in DMF (v/v), DMF. Subsequently, in order to release the protected decapeptide from the resin, 4 resin volumes of a freshly prepared cleavage mixture (1% TFA, 3% TIS in DCM, v/v) were added. The acidic mixture was incubated for 2 minutes, under mixing, and the solution was filtered with a vacuum pump, into a flask containing 1/5 acidic mixture volume of a freshly prepared basic solution (10% pyridine in methanol, v/v). The peptide elution was checked by TLC analysis (chloroform:MeOH 90:10); each step was repeated until no product was detected in the collected fractions. Visualization of the peptide on TLC plates was performed both by UV and by the ninhydrin test. The fractions containing the product were pooled and then evaporated under reduced pressure up to 5% of the volume. The protected peptides were extracted in chloroform/water three times, then they were dried under vacuum. The obtained products were transferred to centrifugal tubes and fresh diethyl ether was added to remove the Mtt-TIS adduct from the protected peptides. The tubes were then centrifuged at 3300 rpm for 4 min at 4 °C and the crude peptides were dried under vacuum.

Peptides purity and identity were assessed by analytical RP-HPLC and LC-ESI-MS analysis (Vydac C18, 4.6 mm x 150 mm; 5 μ m; eluents water 0.1% TFA (A), acetonitrile 0.1 % TFA (B) linear

gradient from 50% to 90% B , over 40 min, flow rate: 0.5 mL/min).

Decapeptides and tetradecapeptide chromatograms and the relative mass spectra are reported in Figure S3, S4.

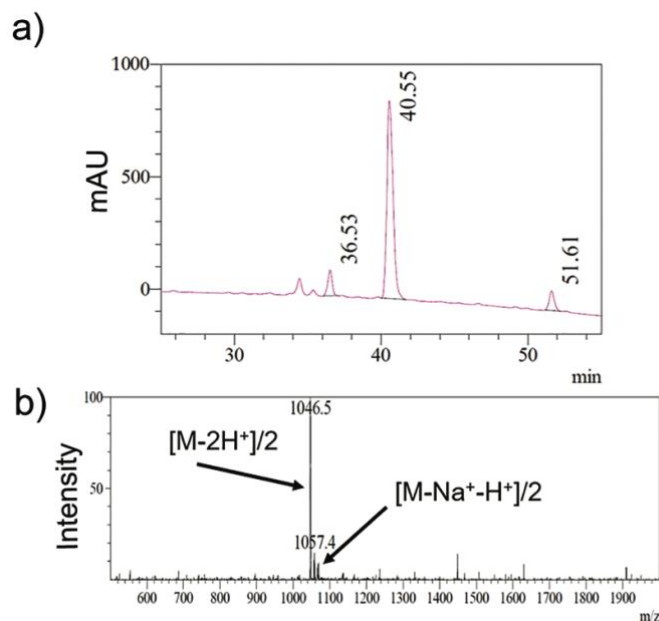


Figure S3. (a) RP-HPLC chromatogram of protected Lys⁹Dab-*D* decapeptide, lacking the Mtt group of Dab⁹ side chain. (b) ESI-MS spectrum relative to the peak at $R_t= 40.55$ min. The mass spectrum was in agreement with the theoretical mass (theoretical mass: 2091.48 Da; observed mass: 2091.0 ± 0.5 Da). The peaks corresponding to the fully protected peptide ($R_t= 51.61$ min) and to the protected peptide lacking the Mtt and Trt protecting groups ($R_t= 36.53$ min) were also identified by mass analysis.

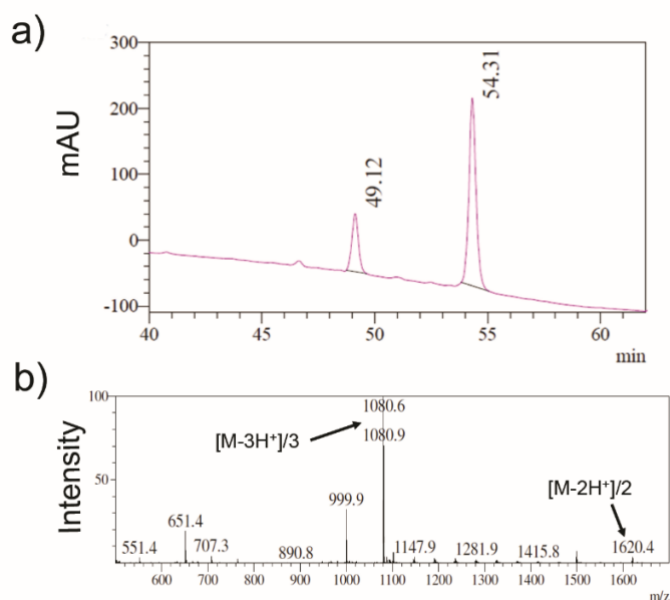


Figure S4. (a) RP-HPLC chromatogram of protected *TD*, lacking the protecting Mmt group of Lys⁹ side chain; (b) ESI-MS spectrum relative to the peak at $R_t= 54.31$ min. The mass spectrum was in agreement with theoretical mass (theoretical mass: 3239.12 Da; observed mass: 3238.8 ± 0.5 Da). The peak corresponding to the protected peptide lacking the Mmt and a Trt protecting groups ($R_t= 36.53$ min) was also identified by mass analysis.

✓ Coupling of decapeptide chain to the Deuteroporphyrin IX

The coupling of decapeptide chain, Lys⁹Dab-**D** to the deuteroporphyrin IX (DPIX) was performed in DMF, in presence of DIPEA (7 eq.), HATU (1 eq.) and deuteroporphyrin IX*2HCl (1.5 eq.) at a final peptide concentration of 0.01 M.

The peptide solution was added drop wise to the deuteroporphyrin solution. The reaction mixture was stirred for 2 h at room temperature, and the pH was checked every 20 min, and adjusted with DIPEA (pH ≈ 8.0), if necessary. The reaction was monitored by analytical HPLC (Vydac C8 column, eluents water 0.1% TFA (A), acetonitrile 0.1 % TFA (B) linear gradient from 50% to 90% B, over 20 min) and by tlc (solvent system: chloroform:MeOH 90:10) until the depletion of starting peptide. The HPLC chromatogram is reported in Figure S5.

Two main peaks were detected, in about 1:1 ratio, both identified as the desired products (Lys⁹Dab-**D**-DPIX monoadducts). The two peaks correspond to two constitutional isomers, due to the coupling of the decapeptide to the propionic group at 2 or 18 position of the DPIX.

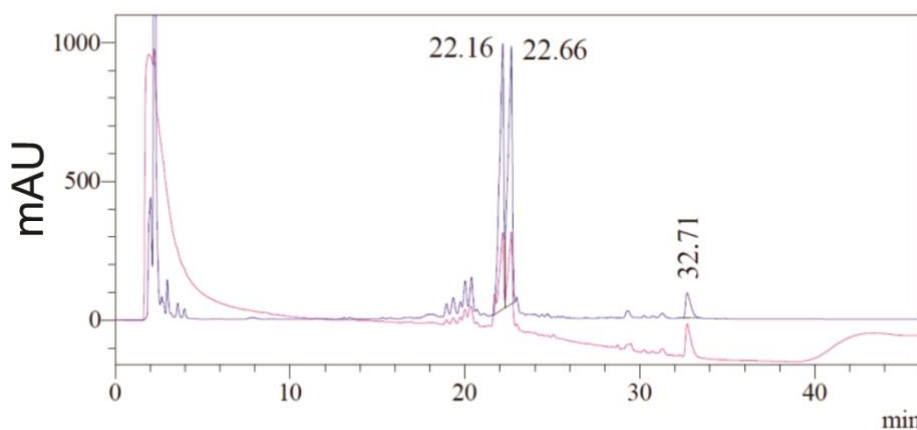


Figure S5. Reaction mixture after 2 hours of the coupling between Lys⁹Dab-**D** and DPIX. The main peaks at Rt = 22.16 min and 22.66 min ($\lambda = 400$ nm blue line, $\lambda = 210$ nm magenta line), correspond to the desired products. The peak at Rt = 32.71 min corresponds to the undesired di-adduct (Lys⁹Dab-**D**)₂-DPIX.

The reaction mixtures were evaporated under reduced pressure and dried. The crude products were purified by Flash Chromatography, on a SNAP HP 100 g silica column, using a chloroform/methanol gradient from 7 to 12% methanol over 6 column volumes, at 50 mL·min⁻¹ flow rate. The products were eluted at 9% methanol, and the pooled fractions containing the desired products were lyophilized. LC-MS analysis confirmed the purity of the products.

✓ Coupling of **TD** to Lys⁹Dab-**D**-DPIX monoadduct and total deprotection of apo-Lys⁹DabMC6*a.

The purified monoadducts (1 eq.) was dissolved in DMF and in presence of DIPEA (6 eq.), HATU (1.2 eq.). Then a solution of **TD** (1.1 eq.) in DMF was added in one portion. The reaction mixture was incubated at room temperature for 2 h. The reaction progress was followed by TLC (eluent: chloroform/methanol 90:10, R_f = 0.65). At the end, the reaction mixture was evaporated under reduced pressure. The protected diadducts were extracted in chloroform/water three times, and the

organic phase was evaporated under reduced pressure and dried.

Hence, the protecting groups were removed by addition of the cleavage mixture (94% TFA, 2.5% EDT, 1% TIS, 2.5% H₂O, v/v). The reaction was conducted under stirring, at 0°C for 1h and at room temperature for other two hours. After concentration on a rotary evaporator, the crude product was precipitated in ice-cold diethyl ether. The mixture was centrifuged (room temperature, at 3300 g), the supernatant was removed and the precipitate was washed twice with three volumes of cold diethyl ether. The precipitate was dried to remove diethyl ether, re-dissolved in water 0.1% TFA and analyzed by LC-MS, using a Vydac C18 column (4.6 mm·150 mm; 5 μm) with a gradient of acetonitrile in 0.1% aqueous TFA, 10% to 50% over 30 min, at 1.0 mL·min⁻¹ flow rate. The crude material was then purified by preparative RP- HPLC (Vydac C18 column, 50 mm·250 mm; 10 μm) at 100 mL·min⁻¹ flow rate, using a gradient of acetonitrile in 0.1% aqueous TFA, 10% to 50% over 50 min. The pooled fractions containing the desired products were lyophilized.

This purification allowed to separate the two apo forms, due to the coupling of the decapeptide at 2 position and of the tetradecapeptide at 18 position of the DPIIX, and *vice versa*.

✓ Metal Insertion

Iron ion was inserted into Lys⁹Dab-**D**-DPIX free bases regioisomer 1 and regioisomer 2 using method the acetate method, slightly modified by us.⁴

Iron (II) acetate (10 eq.) was added to a solution of pure free bases dissolved in an acetic acid/TFE mixture (3 : 2 v/v) ([Lys⁹Dab-**D**-DPIX] = 2.0·10⁻⁴ M) and the reaction mixture was kept at 50 °C for 2 h, refluxing under nitrogen. The reaction was monitored by analytical HPLC, using a Vydac C18 column, with an elution gradient of acetonitrile in 0.1% aqueous TFA, 10% to 50% over 30 min, at 1.0 mL·min⁻¹ flow rate. Once the reaction was completed, the solvent was removed under vacuum and the product re-dissolved in water 0.1% TFA (10 mL) and purified from the excess of Fe (II) acetate by reverse phase-flash chromatography, on a SNAP KP-C18-HS 30 g column, using a gradient of water/0.1% TFA (A) and acetonitrile/0.1% TFA (B), 5% to 95% B over 20 min, flow rate 25 mL min⁻¹.

Lyophilization of the collected fractions afforded the final products (yield 48%). LC-MS analysis confirmed the purity of the products and the expected molecular weight. The analytical chromatograms recorded at λ = 210 nm (magenta line) and at λ = 387 nm (brown line) are reported in Figures S6, S7.

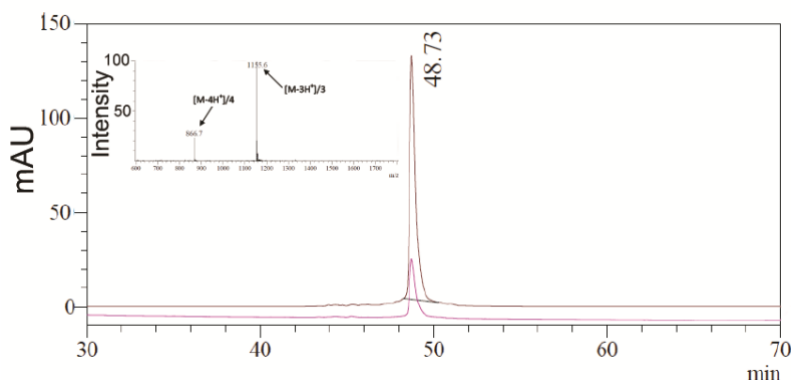


Figure S6. RP-HPLC chromatogram and ESI-MS spectrum of pure Fe-Lys⁹Dab-MC6*a-1 (λ=210 nm, magenta line; λ=400 nm brown line).

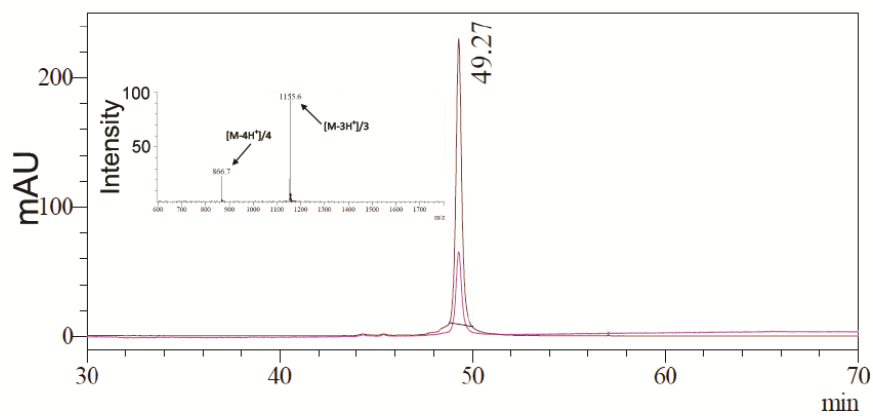


Figure S7. RP_HPLC chromatogram and ESI-MS spectrum of pure Fe-Lys⁹Dab-MC6*a-2 ($\lambda=210$ nm, magenta line; $\lambda=400$ nm brown line).

Section S3: CD Analysis

The secondary structure of Fe-Lys⁹Dab-MC6*a-1 and 2 and its dependence on TFE content was investigated by circular dichroism (CD) in the far-UV region (260-190 nm) (Figure S8).

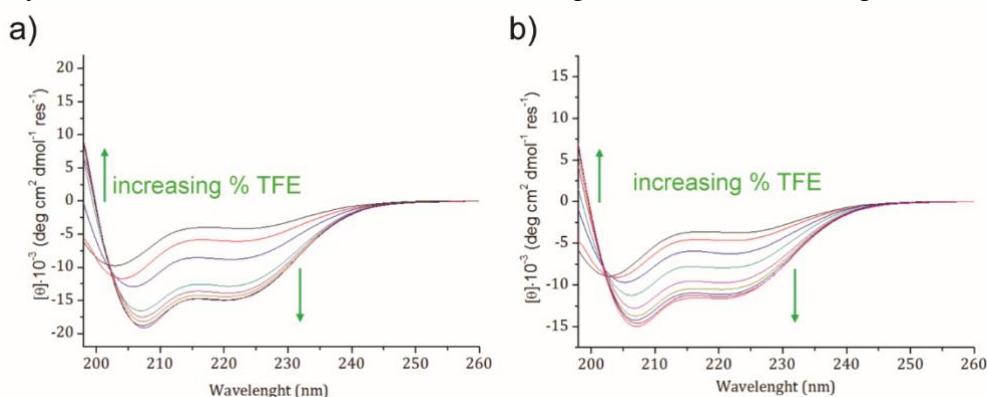


Figure S8. Far-UV CD spectra of Fe-Lys⁹Dab-MC6*a-1 (5.0 10⁻⁶ M) (a) and Fe-Lys⁹Dab-MC6*a-2 (5.0 10⁻⁶ M) (b) in phosphate buffer (20 mM, pH = 5.0) at different TFE concentrations.

The TFE is a co-solvent known for its capability to stabilize helical structure in peptides.⁵⁻⁷ For both isomers, the spectra at higher TFE content are characterized by a negative band around 222 nm (amide transition n-π*), a negative band between 203-207 nm (amide transition π-π*) and a positive band around 190 nm (amide transition π-π*, perpendicular coupling), which are all characteristic features of a helical arrangement of the peptide chains.⁸

In particular, the peptide chains, poorly structured in water, fold into a helix upon addition of 35% TFE (v/v) at pH 5.0. In Table 1 and 2 the main parameters of the far-UV CD spectra are reported.

Table S1. Parameters of the far-UV CD spectra of Fe-Lys⁹Dab-MC6*a-1 in phosphate buffer 20 mM at pH 5.0, at different TFE concentrations (v/v).

%TFE	$[\theta]_{\min} \cdot 10^{-4}$ (deg cm ² dmol ⁻¹ res ⁻¹)	$[\theta]_{222} \cdot 10^{-3}$ (deg cm ² dmol ⁻¹ res ⁻¹)	$[\theta]_{\text{ratio}}$	λ_0 (nm)
0	-0.976 (202.8)	-4.159	0.43	193.8
5	-1.171 (204.0)	-6.083	0.52	194.6
10	-1.292 (205.8)	-8.793	0.68	197.8
20	-1.657 (207.0)	-12.79	0.77	199.4
25	-1.752 (207.2)	-13.81	0.79	199.6
30	-1.818 (207.2)	-14.32	0.79	199.6
40	-1.881 (207.2)	-14.80	0.79	199.8
50	-1.913 (207.4)	-14.84	0.78	199.8

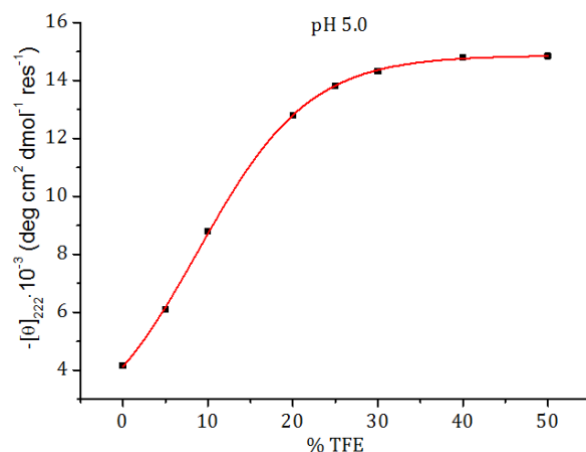


Figure S9. Plot of the molar ellipticity for residue at 222 nm as function of TFE percentage (v/v) of Fe-Lys⁹Dab-MC6*a-1 ($5.0 \cdot 10^{-6}$ M) in phosphate buffer 20 mM at pH 5.0.

Table S2. Parameters of the far-UV CD spectra of Fe-Lys⁹Dab-MC6*a-2 in phosphate buffer 20 mM at pH 5.0, at different TFE concentrations (v/v).

%TFE	$[\Theta]_{\min} \cdot 10^{-4}$ (deg cm ² dmol ⁻¹ res ⁻¹)	$[\Theta]_{222} \cdot 10^{-3}$ (deg cm ² dmol ⁻¹ res ⁻¹)	$[\Theta]_{\text{ratio}}$	λ_0 (nm)
0	-0.893 (202.8)	-3.700	0.41	193.4
5	-0.910 (203.8)	-4.661	0.51	194.6
10	-0.969 (205.2)	-6.262	0.65	197.6
15	-1.123 (206.2)	-7.897	0.70	198.6
20	-1.279 (206.8)	-9.680	0.76	199.2
25	-1.373 (207.0)	-10.47	0.76	199.6
30	-1.423 (207.0)	-11.07	0.78	199.6
40	-1.460 (207.2)	-11.33	0.78	199.6
50	-1.498 (207.2)	-11.55	0.77	199.6

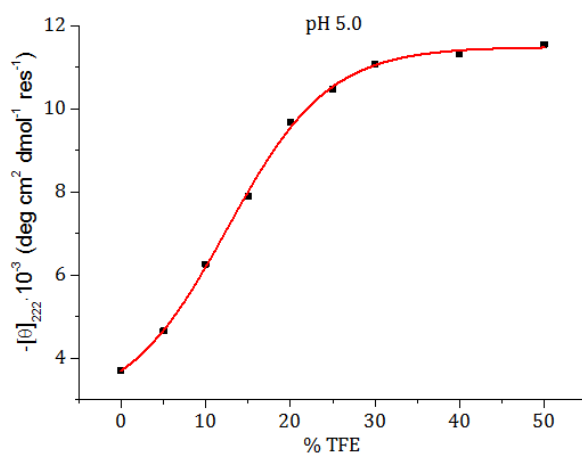


Figure S10. Plot of the molar ellipticity for residue at 222 nm as function of TFE percentage (v/v) of Fe-Lys⁹Dab-MC6*a-2 ($5.0 \cdot 10^{-6}$ M) in phosphate buffer 20 mM at pH 5.0.

In order to elucidate the peptide-heme interactions in the sandwiched three-dimensional structure, the CD spectra of the two compounds were acquired also in the Soret region (460-300 nm).

The CD spectra in the Soret region of both isomers at pH 5 display a negative induced Cotton effect, centered at about 387 nm, whose intensity increases by increasing the TFE concentration (Figure S11)

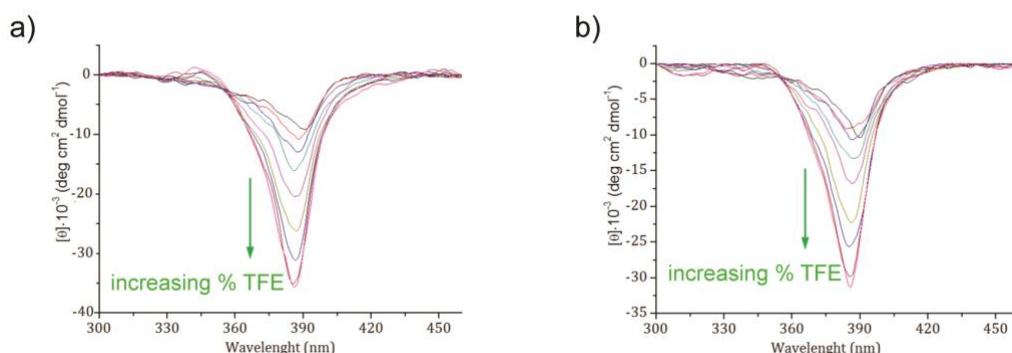


Figure S11. CD spectra in the Soret region of Fe-Lys⁹Dab-MC6*a-1 ($1.5 \cdot 10^{-5}$ M) (a) and Fe-Lys⁹Dab-MC6*a-2 ($1.5 \cdot 10^{-5}$ M) (b) in phosphate buffer (10 mM, pH = 5.0) at different TFE concentrations.

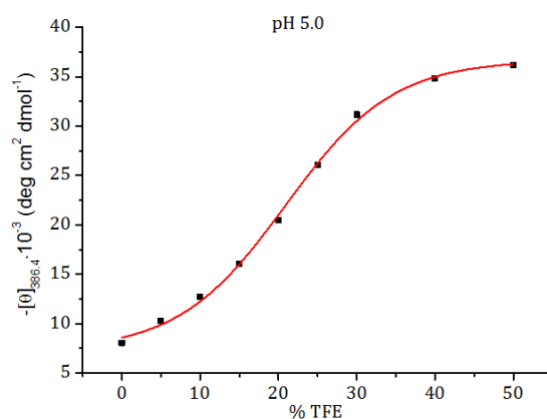


Figure S12. Plot of the molar ellipticity at 386.4 nm as function of TFE percentage (v/v) of Fe-Lys⁹Dab-MC6*a-1 ($1.5 \cdot 10^{-5}$ M) in phosphate buffer 10 mM at pH 5.0.

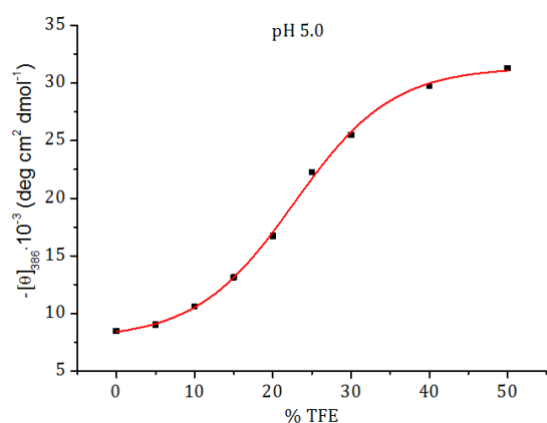


Figure S13. Plot of the molar ellipticity at 386.4 nm as function of TFE percentage (v/v) Fe-Lys⁹DabMC6*a-2 ($1.5 \cdot 10^{-5}$ M) in phosphate buffer 10 mM at pH 5.0.

In order to confirm the sandwiched topology, the CD spectra in the Soret region were acquired also for the cyanide-bound complexes.

The CD spectra in the Soret region of both isomers at pH 5.5 in the presence of 1.5 mM KCN and 40% TFE display a negative induced Cotton effect, centered at about 400 nm (Figure S14).

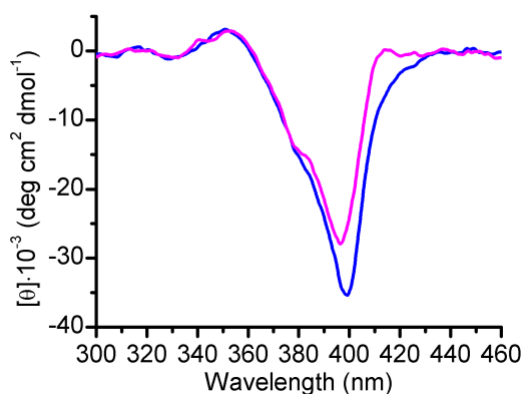


Figure S14. CD spectra in the Soret region of Fe-Lys⁹Dab-MC6*a-1 ($1.5 \cdot 10^{-5}$ M) (blue) and Fe-Lys⁹Dab-MC6*a-2 ($1.5 \cdot 10^{-5}$ M) (magenta) in phosphate buffer (10 mM, pH = 5.5) at 40% (v/v) TFE.

Section S4: NMR characterization

NMR analysis was performed in phosphate buffer (60 mM, pH 5.8)/TFE solution (60/40, v/v) at 299.5 K. NMR samples of Fe-Lys⁹Dab-MC6*a-1 and Fe-Lys⁹Dab-MC6*a-2 were prepared by dissolving weighted amounts of the compounds in the solvent system (V = 0.600 ml) to get the desired concentration. Both complexes show, in this experimental condition, similar spectra. The 1D spectrum of Fe-Lys⁹Dab-MC6*a-1 is reported in Figure S15.

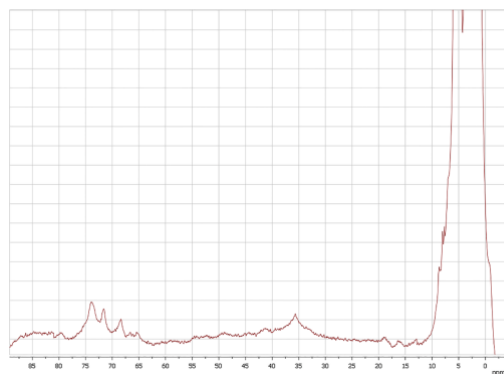


Figure S15. 1D proton NMR spectrum of Fe-Lys⁹Dab-MC6*a-1 ($3.0 \cdot 10^{-4}$ M) in phosphate buffer (60 mM, pH 5.8)/TFE solution (60/40, v/v).

The spectrum is characteristic of high-spin $S = 5/2$ ferriheme-proteins. It shows several peaks shifted out of the diamagnetic region, due to the effect of the paramagnetic ferric ion.

Unfortunately, the NMR signals are very broad and in order to simplify the NMR characterization, we set out to induce the formation of a low spin species, by using exogenous ligands, such as azide and cyanide.

The NMR samples with exogenous ligands were prepared by adding either NaN₃ or KCN aqueous solutions directly in the NMR tubes to reach a final concentration of 0.8 M and 0.02 M, respectively.

Binding of cyanide produced low-spin ($S=1/2$) Fe(III) complexes with spectra suitable for NMR analysis (Figures S16).

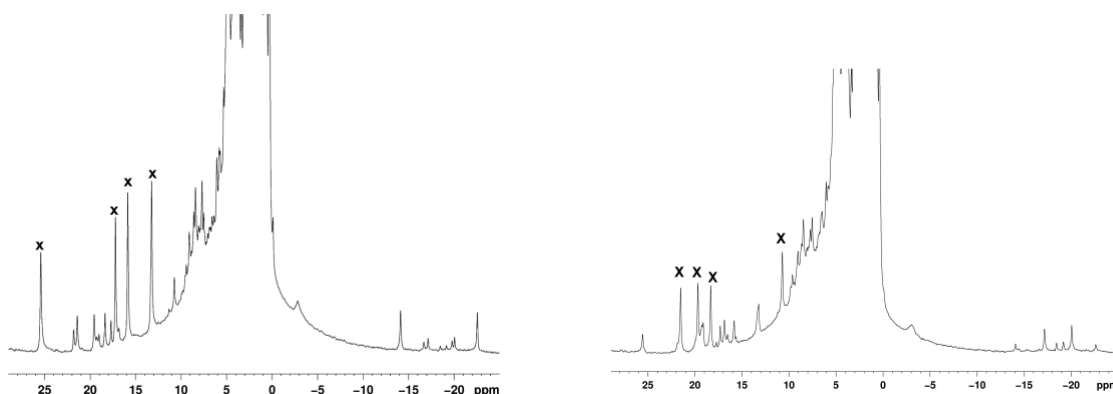


Figure S16. 1D proton NMR spectrum of Fe-Lys⁹Dab-MC6*a cyanide complex, isomer 1 ($3.0 \cdot 10^{-4}$ M) (left) and isomer 2 ($3.5 \cdot 10^{-4}$ M) (right) in phosphate buffer (60 mM, pH 5.8)/TFE solution (60/40, v/v) and 20 mM KCN. Methyl resonances are indicated with X.

In particular, four resonances in the region spanning from 10 to 30 ppm could be assigned to the heme methyl substituents.

Cross peaks were observed in the 2D NOESY spectrum (Figure S17), and, we were able to assign the ^1H shifts of the porphyrin methyls.

The assignment was performed starting from the 5-meso proton.

For cyanide Fe-Lys⁹Dab-MC6*a-1 cyanide complex the 5-meso proton resonates at $\delta = 1.31$ ppm: it is the only proton in dipolar contact with the two methyl groups, 7-CH₃ and 3-CH₃ at 13.2 ppm and 25.5 ppm, respectively (Figure S17). The methyl resonance at 15.8 ppm exhibits dipolar connectivities to a signal at 1.63 ppm (15-meso) and to two protons at about 4 ppm (reasonably attributed to the propionic methylene protons), and therefore it was attributed to the methyl groups at positions 17. Finally, the resonance at 17.2 was attributed to methyl at position 12; this methyl group is in dipolar contact with the 10-meso proton at $\delta = 0.18$ ppm.

In addition, the ^1H - ^{13}C Heteronuclear Multiple Quantum Coherence (HMQC) NMR spectrum was collected, in order to assign the ^{13}C resonance of the porphyrin methyls, which fall in a characteristic region of the spectrum.

The same criteria was used to assign the deuterioporphyrin signals of Fe-Lys⁹Dab-MC6*a-2 cyanide complex.

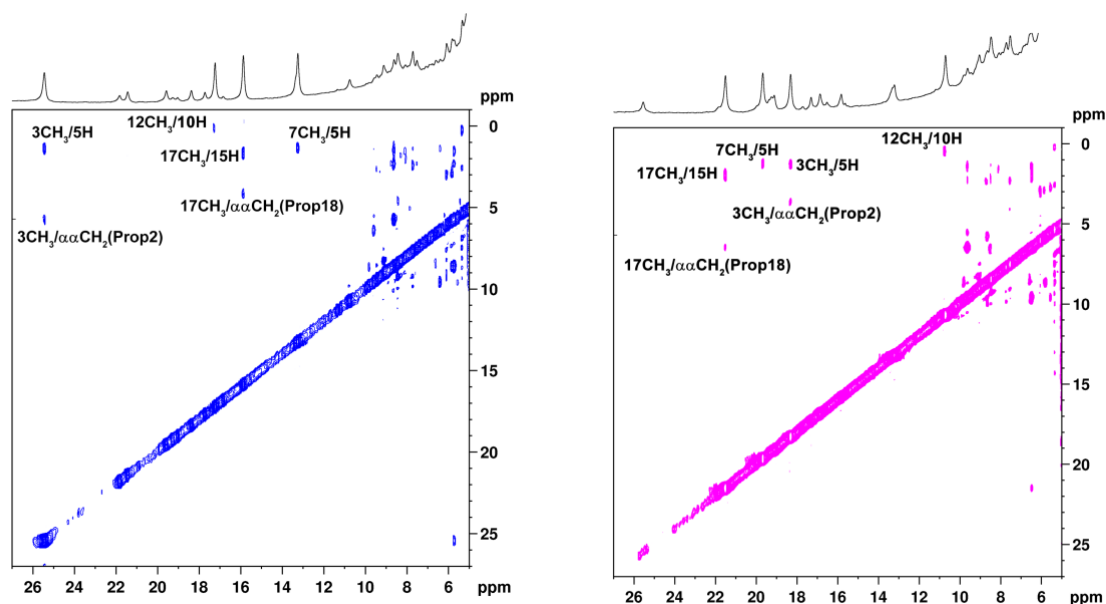


Figure S17. 2D-NOESY spectrum of Fe-Lys⁹Dab-MC6*a cyanide complex, isomer 1 (left) and isomer 2 (right). The NOE connectivities of the DPIX methyls are explicitly labeled.

Section S5: Binding Properties by UV-Vis spectroscopy

✓ *Binding of Fe-Lys⁹Dab-MC6*a-1 and Fe-Lys⁹Dab-MC6*a-2 with exogenous ligands.*

The metal binding properties of Fe-Lys⁹DabMC6*a-1 and 2 were studied by UV-visible spectroscopy (data showed in Figures S18, S19).

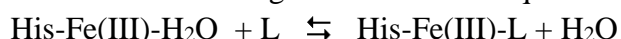
In order to obtain ferric low-spin hexacoordinated complexes helpful for an effective NMR structural characterization, stoichiometric titration of isomer 1 and 2 by small exogenous ligands, azide and cyanide, was carried out by monitoring UV-visible spectral changes in the Soret region.

In particular, changes to the absorption spectra of the regioisomers upon addition of azide and cyanide were monitored between 330 and 450 nm. Sample concentrations were $6.6 \cdot 10^{-6}$ M.

Aqueous KCN stock solutions (0.68 M for Fe-Lys⁹DabMC6*a-1 and 0.87 M for Fe-Lys⁹DabMC6*a-2) were opportunely diluted to perform titration studies, in the concentration range 0 - 6 mM. Following each addition, the mixture was mixed for 5 min, and its UV-vis spectrum was acquired at 25 °C.

Aqueous NaN₃ stock solutions (5 M for both regioisomers) were opportunely diluted to perform titration studies, in the concentration range 0 - 1 M. Following each addition, the mixture was mixed for 5 min, and its UV-vis spectrum was acquired at 25 °C.

This analysis allowed us to evaluate the binding constant for the equilibrium:



and as consequence to estimate the ligand concentration at which saturation occurs. Absorption data points have been fitted with the following binding model:

$$A = \frac{K_a A_\infty [L] + A_0}{(1 + K_a [L])}$$

where K_a is the association constant, A_∞ is the absorption of the complex at infinite concentration of $[L]$ and A_0 is the absorption of the starting aqua-complex.

Azide titration of Fe-Lys⁹Dab-MC6*a-1 and Fe-Lys⁹Dab-MC6*a-2 demonstrated the formation of a complex with dissociation constants of 0.013 M^{-1} and 0.014 M^{-1} , respectively. Cyanide titration of Fe-Lys⁹Dab-MC6*a-1 and Fe-Lys⁹Dab-MC6*a-2 demonstrated the formation of a complex with dissociation constants of $1.5 \cdot 10^{-4} \text{ M}^{-1}$ and $1.2 \cdot 10^{-4} \text{ M}^{-1}$, respectively.

Azide and cyanide titrations cause a red shifted of the Soret band that can be inferred to the binding of the exogenous ligands on the iron(III) axial positions and to the formation of hexacoordinated ferric complexes.

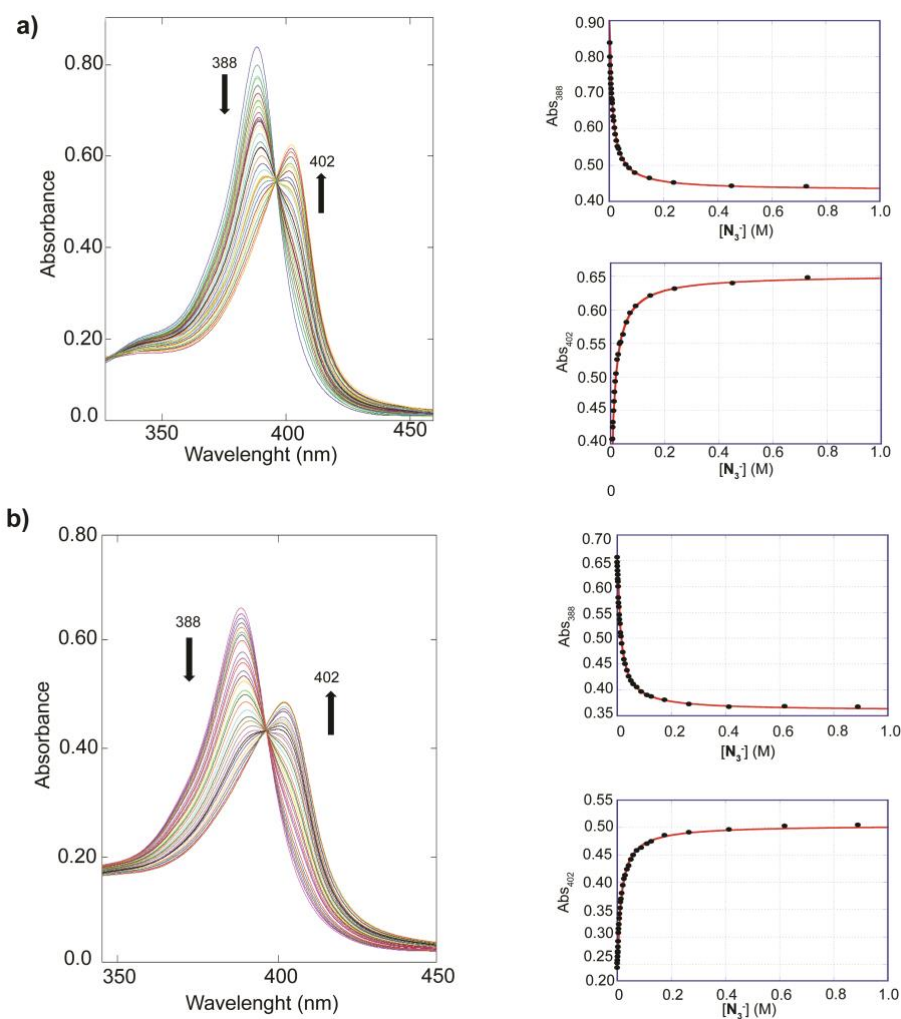


Figure S18. Binding of azide to Fe-Lys⁹Dab-MC6*a complexes. UV-Vis spectra and spectral changes that accompany the addition of the sodium azide in phosphate buffer (pH = 5.8, 60 mM)/TFE, 60/40 (v/v) for Fe-Lys⁹Dab-MC6*a-1 ($6.6 \cdot 10^{-6}$ M) (a) and for Fe-Lys⁹Dab-MC6*a-2 ($6.6 \cdot 10^{-6}$ M) (b), respectively. Arrows indicate changes of the Soret band upon azide addition. The plots of the absorbance at 388 and 402 nm as function of azide concentration are also reported. The black dots are the experimental data, which have been fitted with a single binding model (red line).

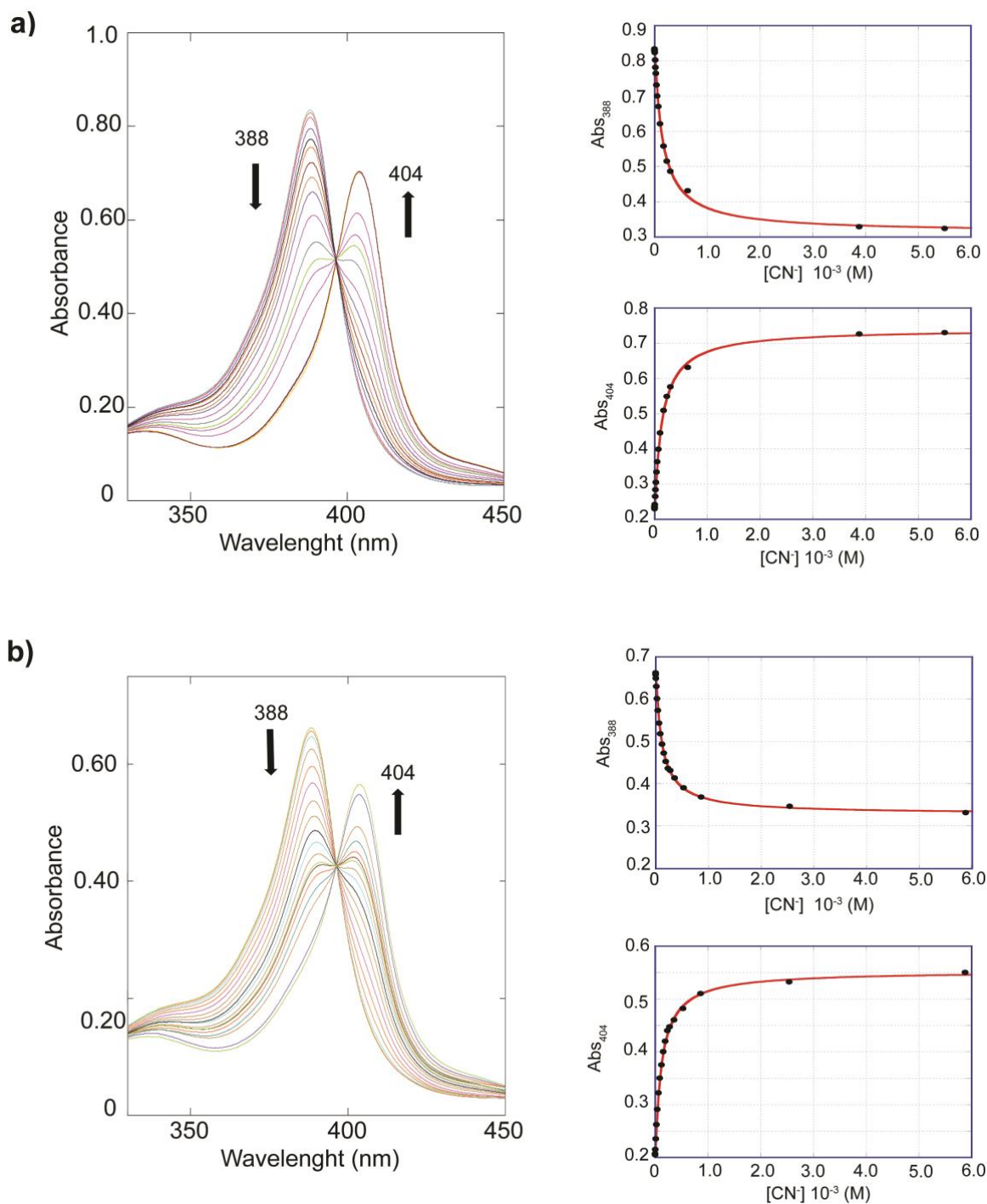


Figure S19. Binding of cyanide to Fe-Lys⁹Dab-MC6*a complexes. UV-Vis spectra and spectral changes that accompany the addition of the KCN in phosphate buffer (pH = 5.8, 60 mM)/TFE, 60/40 (v/v)) for Fe-Lys⁹Dab-MC6*a-1 ($6.6 \cdot 10^{-6}$ M) (a) and for Fe-Lys⁹Dab-MC6*a-2 ($6.6 \cdot 10^{-6}$ M) (b), respectively. Arrows indicate changes of the Soret band upon cyanide addition. The plots of the absorbance at 388 and 404 nm as function of cyanide concentration are also reported. The black dots are the experimental data, which have been fitted with a single binding model (red line).

Section S6: Stopped-Flow kinetic analysis

The initial rates of ABTS oxidation (v_0) are plotted as a function of both substrates concentration (Figures S20 and S21). Data were fitted according to Michaelis-Menten kinetics equation.

Enzyme concentration in all experiments was fixed at $2.0 \cdot 10^{-8}$ M for both Fe-Lys⁹Dab-MC6*a-1 and 2. Mimochrome stock solutions were prepared in acidic water (0.1% TFA, v/v) and diluted to the final concentration in the reaction buffer (50 mM phosphate/TFE (1:1 v/v), pH 6.5).

ABTS and H₂O₂ stock solutions were prepared as previously described.¹

K_m values for ABTS and H₂O₂ were measured keeping one of the two substrate concentration constant while varying the other and *vice versa*. For the determination of $K_m^{H_2O_2}$, ABTS concentration was fixed at 2.0 mM while H₂O₂ was varied from 0 to 200 mM. For the determination of K_m^{ABTS} , H₂O₂ concentration was fixed at 450 mM while ABTS concentration was varied from 0 to 0.33 mM.

Pro-Data SX program was used for system control and to extract the initial rates of ABTS oxidation (v_0 , mM s⁻¹). v_0 values were plotted as a function of both substrates concentration and data points fitted according to the Michaelis and Menten equation, using Kaleidagraph 4.1 software:

$$v = \frac{v_{max}[S]}{K_m + [S]}$$

From data fitting, K_m and k_{cat} values were calculated (Table S3).

Table S3. Fe-Lys⁹Dab-MC6*a-1 and 2 steady-state kinetic parameters. Fe-MC6*a and HRP parameters are reported for comparison.

Enzyme	K_m H ₂ O ₂ (mM)	K_m ABTS (10 ⁻² mM)	k_{cat} (10 ³ s ⁻¹)	k_{cat}/K_m H ₂ O ₂ (10 ³ mM ⁻¹ s ⁻¹)	k_{cat}/K_m ABTS (10 ³ mM ⁻¹ s ⁻¹)	ref
Fe-Lys ⁹ Dab-MC6*a-1	204±8	2.8±0.1	1.00±0.02	0.0049±0.0003	36±2	this work
Fe-Lys ⁹ Dab-MC6*a-2	234±19	27±2	3.0±0.2	0.013±0.002	11±2	this work
Fe-MC6*a	440±50	9±1	5.8±0.3	0.013±0.002	64±8	1
HRP	0.93±0.05	70±8	2.70±0.03	2.9±0.2	3.8±5	1

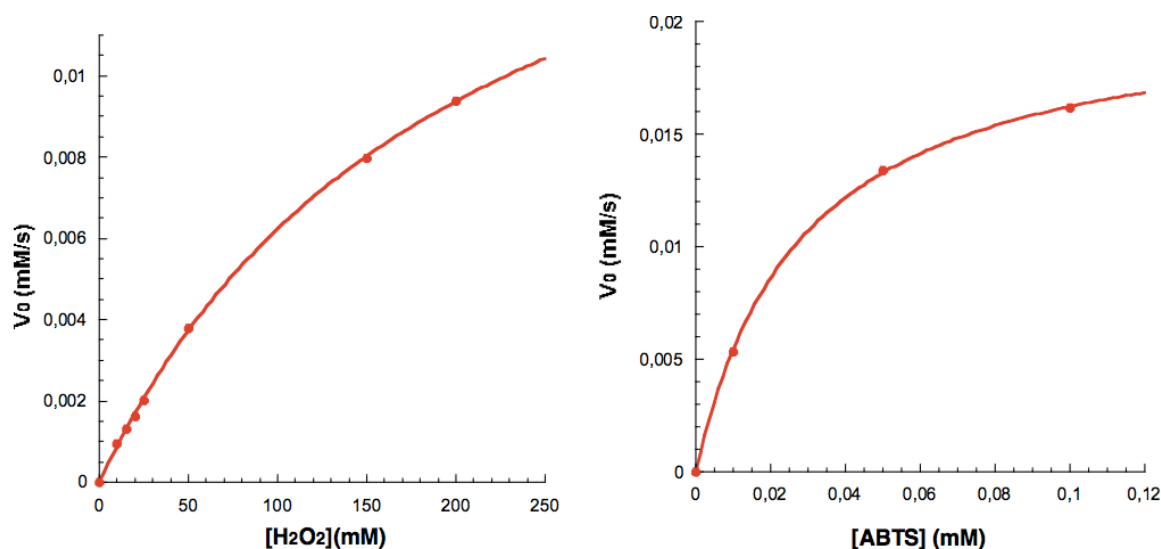


Figure S20. Peroxidase-like activity of Fe-Lys⁹Dab-MC6*a-1. Initial rate dependence towards H₂O₂ concentration (left): reaction conditions were Fe-Lys⁹Dab-MC6*a-1 (20 nM), ABTS (2 mM) in 50 mM phosphate buffer pH 6.5/TFE (1:1 v/v). Initial rate dependence towards ABTS concentration (right): reaction conditions were Fe-Lys⁹Dab-MC6*a-1 (20 nM), H₂O₂ (500 mM) in 50 mM phosphate buffer pH 6.5/TFE (1:1 v/v).

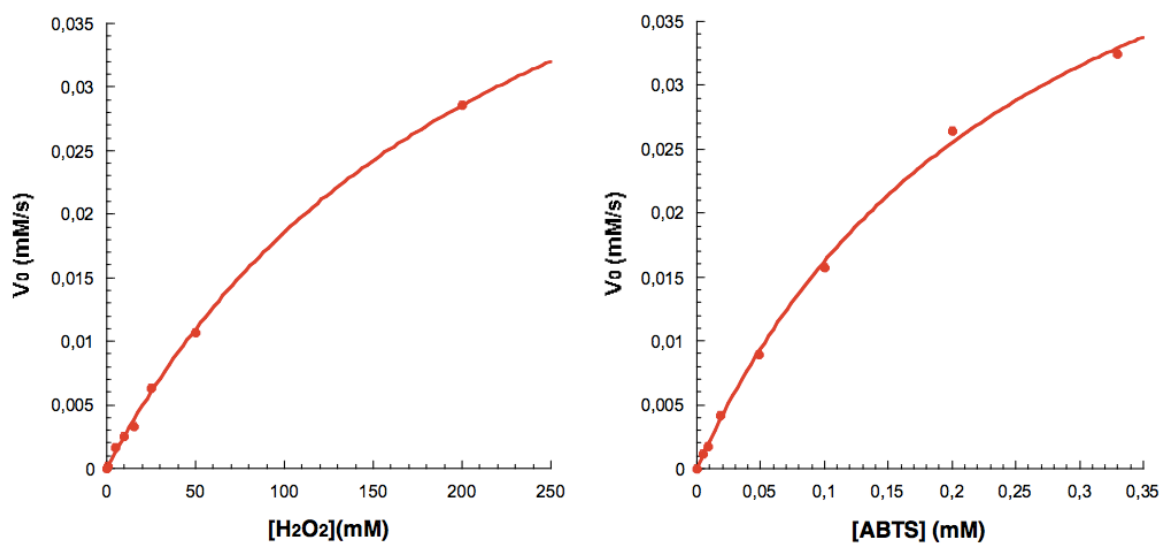


Figure S21. Peroxidase-like activity of Fe-Lys⁹Dab-MC6*a-2. Initial rate dependence towards H₂O₂ concentration (right): reaction conditions were Fe-Lys⁹Dab-MC6*a-2 (20 nM), ABTS (2 mM) in 50 mM phosphate buffer pH 6.5/TFE (1:1 v/v). Initial rate dependence towards ABTS concentration (left): reaction conditions were Fe-Lys⁹Dab-MC6*a-2 (20 nM), H₂O₂ (500 mM) in 50 mM phosphate buffer pH 6.5/TFE (1:1 v/v).

Section S7: References

- 1 G. Caserta, M. Chino, V. Firpo, G. Zambrano, L. Leone, D. D'Alonzo, F. Nistri, O. Maglio, V. Pavone and A. Lombardi, *ChemBioChem*, 2018, **19**, 1823-1826.
- 2 C. Vicari, I. H. Saraiva, O. Maglio, F. Nistri, V. Pavone, R. O. Louro and A. Lombardi, *Chem. Commun.*, 2014, **50**, 3852-3855.
- 3 P. Sieber, *Tetrahedron Lett.*, 1987, **28**, 2107-2110.
- 4 F. Nistri, A. Lombardi, G. Morelli, O. Maglio, G. D'Auria, C. Pedone and V. Pavone, *Chem. Eur. J.*, 1997, **3**, 340-349.
- 5 M. Goodman, I. Listowsky, Y. Masuda and F. Boardman, *Biopolymers*, 1963, **1**, 33-42.
- 6 J. W. Nelson and N. R. Kallenbach, *Proteins Struct. Funct. Bioinformatics*, 1986, **1**, 211-217
- 7 A. Jasanoff and A. R. Fersht, *Biochemistry*, 1994, **33**, 2129-2135.
- 8 N. J. Greenfield and G. D. Fasman, *Biochemistry*, 1969, **8**, 4108-4116.